Sonochemical Synthesis of Nanophase Indium Sulfide

S. Avivi (Levi),[†] O. Palchik,[†] V. Palchik,[‡] M. A. Slifkin,[‡] A. M. Weiss,[‡] and A. Gedanken*,[†]

Department of Chemistry, Bar-Ilan University, Ramat-Gan, 52900 Israel, and Department of Electronics, Jerusalem College of Technology, Jerusalem, 91160 Israel

Received February 8, 2001

The sonication of $InCl_3$ with thioacetamide in an aqueous solution has led to different products, depending on the sonication temperature. Sonication at 0 °C yielded In_2O_3 as the major product and In_2S_3 as a minor component. On the other hand, when the reaction is carried out at "room temperature", nanocrystalline In_2S_3 is obtained as the sole product. The products of sonication at 0 °C are obtained in the amorphous form. An explanation for this is offered based on the hot spot mechanism.

Introduction

β-In_2S_3 (body-centered tetragonal) is an n-type semiconductor with a band gap of 2.0−2.3 eV, giving it photoconductive properties.[1] This, together with its luminescence properties, makes the material a promising optoelectronic material. β-In_2S_3 has already inspired applications in the preparation of green and red phosphors in the manufacture of picture tubes for color televisions,[2,3] dry cells,[4] and heterojunction for use in photovoltaic electric generators.[5] Indium sulfide exists in three different forms: a defect cubic structure known as α-In_2S_3, a defect spinel, β-In_2S_3, which is stable above 420 °C, and a layered structure, γ-In_2S_3, which is stable above 754 °C.[6−8] Despite this distinction between the phases, the defect cubic form has been referred to, in a few papers, as a β-In_2S_3 phase.[1,2]

The methods by which In_2S_3 was prepared include a direct reaction of the elements in a quartz container at a high temperature,[9] heat treatment of In_2O_3 in H_2S at elevated temperatures,[10,11] and the metathesis reaction of $InCl_3$ and Li_2S at 500 °C.[12] Wet chemical methods have also been applied to prepare indium sulfide, including a precipitation reaction wherein In_2S_3 was precipitated from an aqueous solution of $InCl_3$ by H_2S,[13] $(NH_4)_2S$,[5] or NaHS.[14] A detailed survey of all the other wet chemical methods can be found in Yu's paper.[2] For its use in solar cells, thin film deposition techniques such as organometallic CVD,[15] spray pyrolysis,[16] ALE (atomic layer epitaxy),[1] and CBD (chemical bath deposition)[17] have been developed. Finally, a hydrothermal reaction[2] of $InCl_3$ and sodium sulfide at 140 °C yielded 13-nm spherical shape particles.

In the current paper we report on the preparation of nanophased indium sulfide by sonicating an aqueous solution of indium chloride and thioacetamide, the latter serving as the sulfur source. The reaction was carried out at different temperatures, and while at 0 °C an amorphous product is obtained, a crystalline In_2S_3 product is fabricated when the reaction is carried out at room temperature. Indium ions were a part of a recent investigation in which the sonohydrolysis of group 13 in the periodic table was studied,[18−20] yielding nanosized needle-shaped $In(OH)_3$ particles.

Experimental Section

An aqueous solution containing 1.0 g of $InCl_3$ (1 M) and 0.4 g (1.2 M) of thioacetamide (CH_3CSNH_2) was placed in a 60-mL cell and was exposed to high-intensity (100 W/cm^2) ultrasound radiation operating at 20 kHz, for 4 h, at room temperature. This was done by direct immersion of a titanium horn (Vibracell, horn diameter 1.13 cm) under argon at a pressure of 1.5 atm. The titanium horn was inserted to a depth

* To whom correspondence should be addressed.
[†] Bar-Ilan University.
[‡] Jerusalem College of Technology.

(1) Asikainen, T.; Ritala, M.; Leskela, M. *Appl. Surf. Sci.* **1994**, *82/83*, 122.
(2) Yu, S.; Shu, L.; Qian, Y.; Xie, Y.; Yang, J.; Yang, L. *Mater. Res. Bull.* **1998**, *33*, 717.
(3) (a) Jpn. Patent Application, *Chem. Abstr.* **1981**, *95*, 107324x. (b) Jpn. Patent Application, *Chem. Abstr.* **1979**, *96*, 113316h. (c) Jpn. Patent. Application, *Chem. Abstr.* **1979**, *91*, 67384a.
(4) Dalas, E.; Kobotiatis, L. *J. Mater. Sci.* **1993**, *28*, 6595.
(5) Dalas, E.; Sakkopoulos, S. *J. Mater. Sci.* **1993**, *28*, 5456.
(6) Rehwald, W.; Harbeke J. *J. Phys. Chem. Solids* **1965**, *26*, 1309.
(7) Diehl, R.; Nitsche, R. *J. Cryst. Growth* **1975**, *28*, 306.
(8) Yu, S.-H.; Shu, L.; Wu, Y.-S.; Yang, J.; Xie, Y.; Qian, Y.-T. *J. Am. Ceram. Soc.* **1999**, *82*, 457.
(9) Kaito, C.; Saito, Y.; Fujita, K. *J. Cryst. Growth* **1989**, *94*, 967.
(10) Hahn, H.; Klinger, W.; *Z. Anorg. Chem.* **1949**, *260*, 97.
(11) Richard, H. B.; William, H. M. *J. Phys. Chem. Solids* **1959**, *10*, 333.
(12) Fitzmaurice, J. C.; Parkin, I. P. *Main Group Met. Chem.* **1994**, *17*, 481.
(13) Stubbs, M. F.; Schufle, J. A.; Thompson, A. J.; Duncan, J. M. *J. Am. Chem. Soc.* **1952**, *74*, 1441.
(14) Kumta, P. N.; Phule, P. P.; Risbud, S. H. *Mater. Lett.* **1987**, *5*, 401.
(15) Nomura, R.; Konishi, K.; Matsuda, H. *Thin Solid Films* **1990**, *198*, 339.
(16) Kim, W.; Kim, C. *J. Appl. Phys.* **1986**, *60*, 2631.
(17) Lokhande, C. D.; Ennaoui, A.; Patil, P. S.; Giersig, M.; Diesner, K.; Muller, M.; Tributsch, H. *Thin Solid Films* **1999**, *340*, 18.
(18) Avivi, S.; Mastai, Y.; Hodes, G.; Gedanken, A. *J. Am. Chem. Soc.* **1999**, *121*, 4196.
(19) Avivi, S.; Mastai, Y.; Hodes G.; Gedanken, A. *Chem. Mater.* **2000**.
(20) Avivi, S.; Mastai, Y.; Hodes G.; Gedanken, A. *J. Am. Chem. Soc.* **2000**.

10.1021/cm010162+ CCC: $20.00
Published on Web 05/26/2001

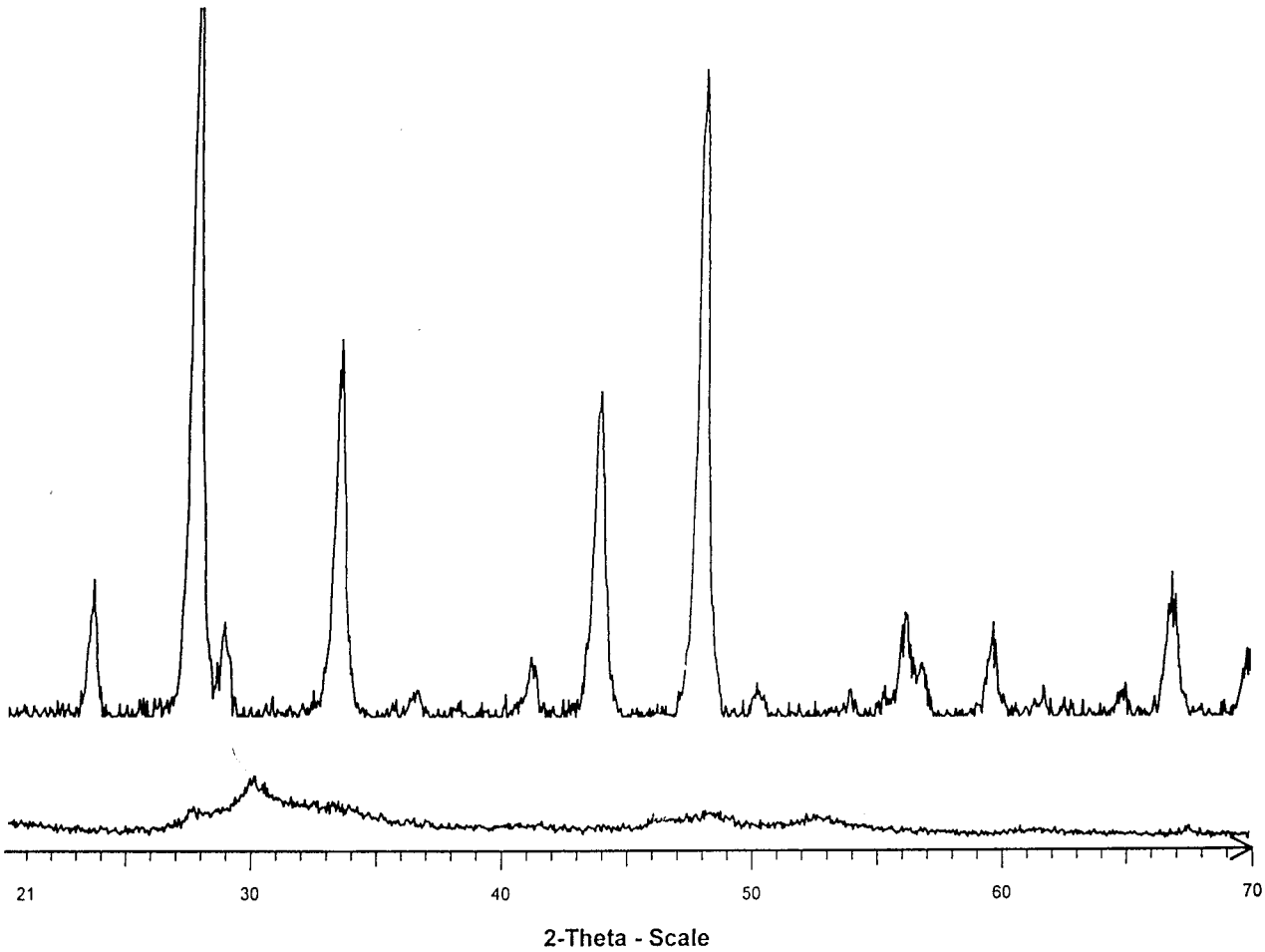

Figure 1. (a) XRD patterns for the material prepared at 0 °C. (b) XRD patterns for the material prepared at room temperature.

of 1 cm in the solution. The reaction cell was not thermostated, and the final temperature was 80 °C. The term "room temperature" will therefore refer to the conditions of nonthermostated sonication. The sonication was also carried out at 0 °C in a thermostated cooling bath.

Powder X-ray diffraction (XRD) patterns were measured using a Bruker D8 advance and Cu Kα irradiation at $\lambda = 1.5406$ Å. Differential scanning calorimetry (DSC) of the dried product was carried out using a Mettler DSC-30 with a heating rate of 10 °C/min under a flow of nitrogen. The morphology of the product was determined by transmission electron microscopy (Philips CM-12) operating at 120 kV. The other measuring instruments have been reported in previous papers.[18−20] Photoacoustic measurements were conducted employing a homemade instrument that has been described elsewhere.[21] The photoacoustic method, which dates back to the time of Alexander Graham Bell, consists of illuminating the sample by chopped monochromatic light in an airtight cell connected to a microphone. The light is absorbed and converted to heat. The chopped heat then flows to the surface of the sample, where it produces an acoustic wave. The signal from the microphone is detected with a lock-in voltmeter. The signal, which is acquired as a function of wavelength, is normalized against the absorption of carbon black powder, the 100% absorber. The instrument operates over the wavelength region 300−1600 nm. The spectrum is independent of the nature of the sample, unlike in reflectance spectroscopy, where the nature of the surface can have a marked effect on the spectrum. This is particularly useful for particulate matter, which causes turbidity and scattering, so that conventional absorption spectroscopy is not very helpful. The method is completely nondestructive. The photoacoustic spectra show features that are much better resolved than those in the absorption spectra of dispersive material.

(21) Slifkin, M. A.; Luria, L.; Weiss, A. M. *SPIE* **1998**, *3110*, 481.

Results

The sonication products were characterized by XRD diffraction measurements. Figure 1 illustrates the diffraction patterns of the 0 °C sonication products (Figure 1a), while the products of the sonication at "room temperature" are depicted in Figure 1b. It is clear that the structureless features detected for the 0 °C reaction (Figure 1a) are due either to their amorphous nature or to their small particle size or to the mixture of amorphous and nanocrystalline In_2S_3. We can see some small broad diffraction peaks at $2\theta = 10.9°$, 27.4°, 29.6°, 47.7°, and 53.1°, which are close to the reported data for β-In_2S_3 (JCPDS card 25-390). The broad nature of the diffraction peaks implies that nanocrystalline β-In_2S_3 has formed. The peaks observed for the room-temperature product match JCPDS card 25-390. These peaks are related to the body-centered tetragonal phase. Using the Debye−Scherrer equation, the size is calculated to about 40 nm. Regarding the products of the 0 °C reaction, a DSC measurement was carried out to check the amorphous nature of the product. The results are presented in Figure 2. The strong exothermic peak detected at about 500 °C is assigned as the crystallization temperature of the amorphous product. The peak disappeared when the sample was reheated over the same temperature range. To further ascertain the amorphous nature of the products, we measured the

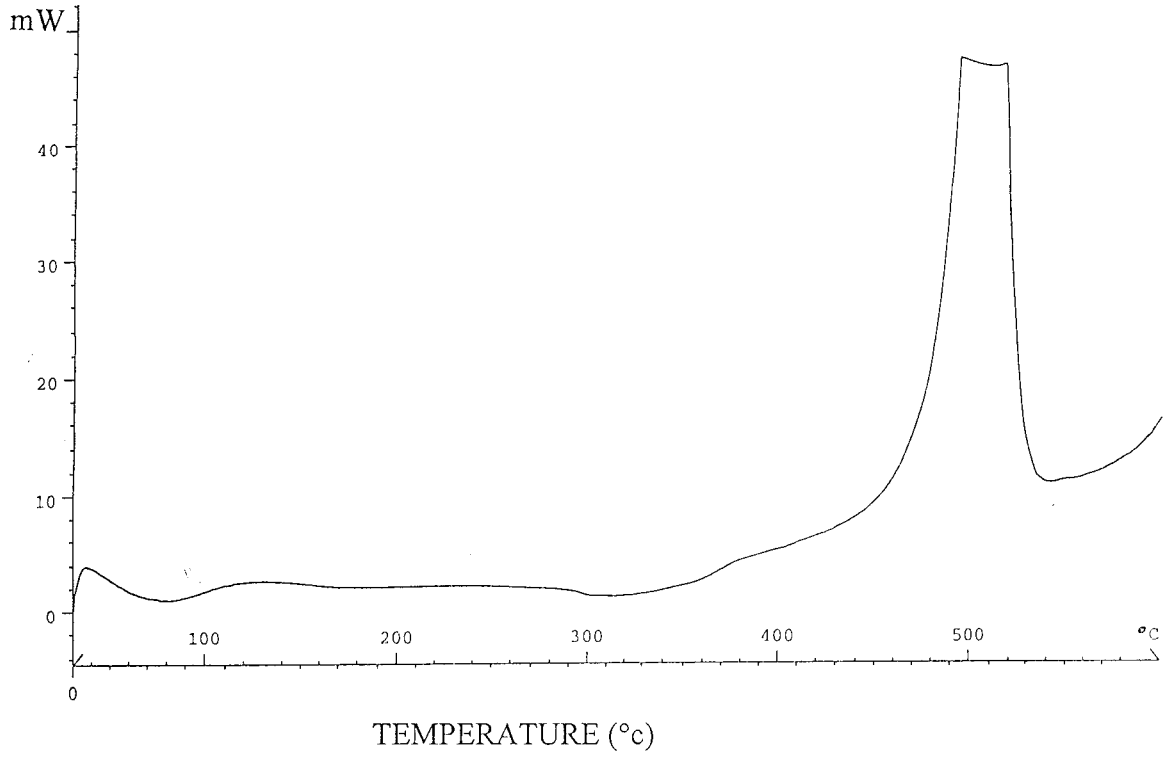

Figure 2. DSC spectrum of the sonication product prepared at 0 °C. The heating rate was 10 °C/min under a flow of argon.

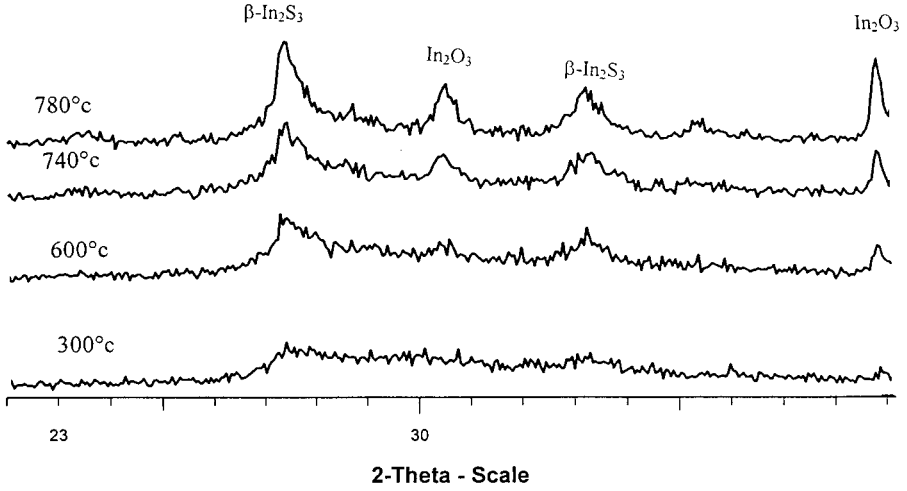

Figure 3. Temperature-dependent X-ray diffraction spectrum of the material prepared at 0 °C. The heating rate was 20 °C/min.

XRD diffraction as a function of temperature (Figure 3). The measurements were carried out over the 20−980 °C temperature range. Every 20 °C a diffraction pattern is measured. The patterns of a body-centered tetragonal In_2S_3 (JCPDS card 25-390) became distinguishable at about 600 °C. Unlike the products of the room-temperature sonication, where only one phase of In_2S_3 is obtained and where no impurities were detected according to the XRD diffraction, the 0 °C heated products reveal In_2O_3 as the major product (JCPDS card 06-416). Although the peaks of the In_2O_3 become distinguishable at a higher temperature than those of the In_2S_3 (740 vs 600 °C), at 980 °C they are clearly more intense than those of In_2S_3. The appearance of the In_2O_3 is not in accordance with our early study of the sonohydrolysis of an aqueous solution of $InCl_3$,[21] where $In(OH)_3$ has been obtained as the only product. The $In(OH)_3$ has been converted to In_2O_3 upon heating.[19] In the current research there is no evidence from the DSC measurements (Figure 2) of the decomposition of $In(OH)_3$ at 290 °C, as observed before.[19] The as-prepared material of the 0 °C reaction is a mixture of amorphous In_2O_3 and In_2S_3. This indicates that while at lower temperature two simultaneous reactions are operative, at higher sonication temperatures the speed of the formation of In_2S_3 is faster than the sonohydrolysis.

The morphologies of the reaction products are also different. In Figure 4 we present the TEM pictures of the room-temperature and 0 °C reaction products. The 0 °C products (Figure 4a) are formed as spherical particles with a size range of 5−20 nm. Only a small degree of aggregation is observed. The room-temperature products (Figure 4b) exhibit a crystalline nature, and their size is greater than the 0 °C products and is estimated as 20−40 nm. This size matches the calculated value from the XRD data by the Debye−Scherrer

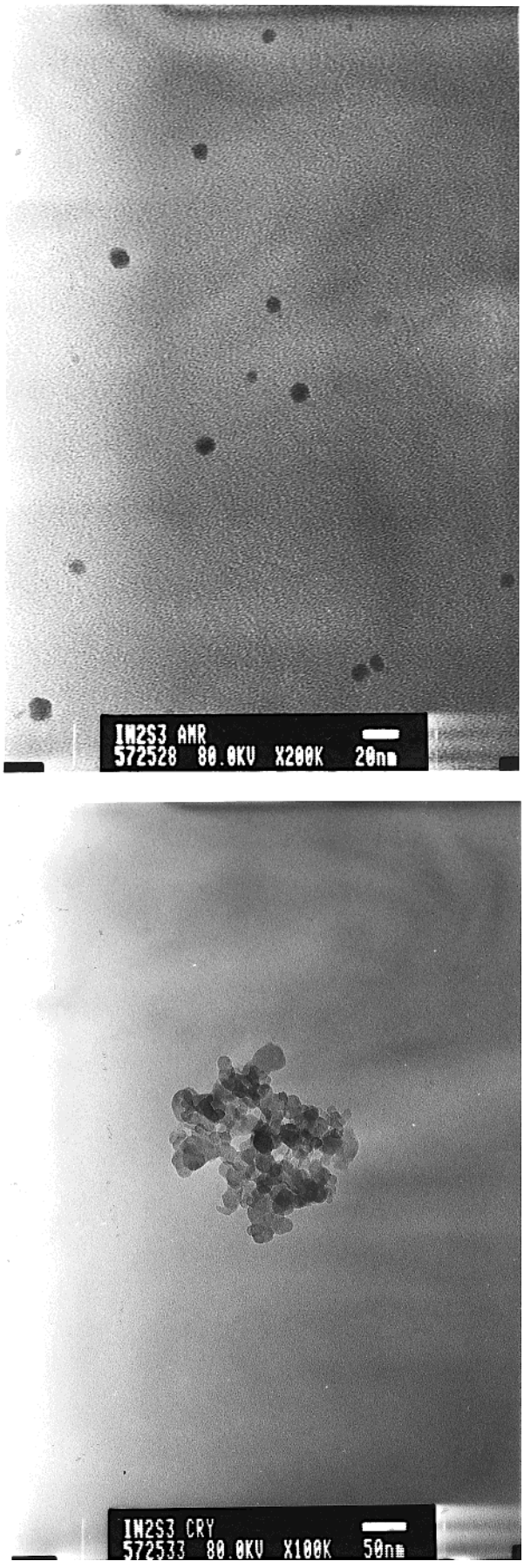

Figure 4. (a) TEM image of the material prepared at 0 °C. Scale: 0.5 cm = 20 nm. (b) TEM image of the material prepared at room temperature. Scale: 0.6 cm = 50 nm.

equation. Aggregation is observed for the room-temperature particles.

The photoacoustic spectra of both room temperature and 0 °C products are shown in Figure 5a,b, respectively. One can see very clear differences between the band edges. For the crystalline product (prepared at room temperature) we have estimated the direct band gap using the "knee" method.[22] The calculated value is 2.34 eV (see Figure 5a). This value is slightly bigger than that in the literature, where the bulk band gap is 2.0−2.3 eV.[1] This is probably due to the size quantization effect, which is generally observed for nanoparticles.[23] The slope of the absorption band is not very steep, and this is due to the relatively low monodispersity of the nanoparticles, which is in very good agreement with TEM and XRD (Scherrer equation) measurements (20−40 nm). We did not observe any other features on this spectrum around the absorption edge. In the case of the amorphous product (prepared at 0 °C), the band gap observed at 2.46 eV is not so clear as in the case of the crystalline product, which is a result of our dealing with a mixture of the compounds as confirmed by XRD. In this case, there is a blue shift even bigger than that in the crystalline case, which results from much smaller dimensions of the nanoparticles in the amorphous samples (5−20 nm from the TEM and XRD measurements). We also observed some absorption features at the higher wavelength segment of the spectrum. At this stage we cannot explain these peaks.

Reaction Mechanism

In the neighborhood of the collapsing bubble there are three regions:[24,25] the center of the collapsing bubble, where the temperature can reach 5000 K; the interface layer, estimated as a 200-nm width ring, where a lower temperature of about 2000 K is measured; and the bulk solution. The reaction that takes place inside the collapsing bubble occurs in the gas phase, whereas in the interface layer a liquid-phase reaction happens. In our discussion we consider $InCl_3$, a nonvolatile compound at room temperature, and the In^{3+} ions will therefore react only in the interfacial region, that is, a room-temperature reaction in which the temperature reaches 80 °C. At this temperature the vapor pressure of the thioacetamide is appreciable, and therefore we propose that the first step, the hydrolysis of the thioacetamide, occurs inside the collapsing bubble:

$$H_2O \text{)))) } H^{\bullet} + OH^{\bullet} \quad (1)$$

$$2H^{\bullet} + CH_3CSNH_2 \rightarrow H_2S + CH_3CNH_2^{\bullet} \quad (2)$$

Equation 1 represents the formation of a primary radical from the ultrasound-initiated dissociation of water. The formation of H_2S via reaction (2), which has

(22) Rosencwaig, A. *Photoacoustics and Photoacoustic Spectroscopy*; Wiley: New York, 1980.
(23) Palchik, O.; Kerner, R.; Gedanken, A.; Weiss, A. M.; Slifkin, M. A. *J. Mater. Chem.*, in press.
(24) Suslick, K. S.; Hammerton, D. A. *IEEE Trans. Ultrason., Ferroelec., Freq. Control* **1986**, UFFC-33, 143.
(25) Suslick, K. S.; Hammerton, D. A.; Cline, R. E. *J. Am. Chem. Soc.* **1986**, *108*, 5641.

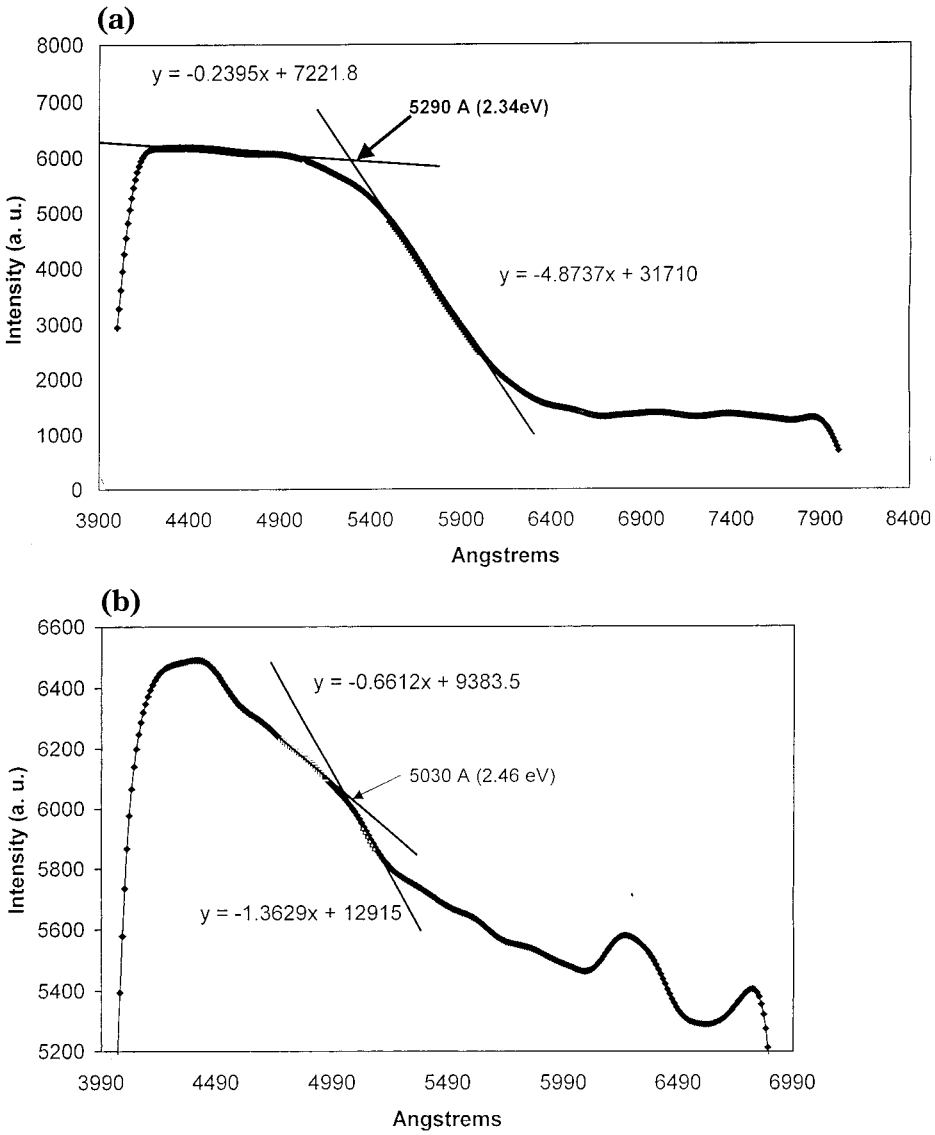

Figure 5. (a) The photoacoustic spectra of the room-temperature product. (b) The photoacoustic spectra of the 0 °C product.

already been suggested by Grieser,[26] further reacted with In^{3+} ions in the interfacial region to yield $In_2S_{3(s)}$:

$$2In^{3+}_{(aq)} + 3H_2S_{(aq)} \rightarrow In_2S_{3(s)} + 6H^+_{(aq)} \qquad (3)$$

Before the reaction the pH solution was 1.48, and after the reaction it was 0.48, which can be understood by reaction (3).

When the reaction is carried out at 0 °C, reaction (2) cannot occur in the gas phase due to the low vapor pressure of the thioacetamide in the collapsing bubble. It is assumed that it might, however, occur in the interface layer. On the other hand, we have already shown that in this layer a competing reaction is also going on:

$$2In^{3+}_{(aq)} + 3H_2O_{(l)} \xrightarrow{)))))} In_2O_{3(s)} + 6H^+_{(aq)} \qquad (4)$$

The hydrolysis was studied at 75 or 85 °C.[27] We have already pointed out that although the hydrolysis of indium salts occurs at relatively low temperatures, it does not occur (without sonication) at temperatures lower than 75 °C. This is only due to the local high temperatures developed during sonication when In_2O_3 or $In(OH)_3$ are obtained. The rate of reaction (4) in the interface layer is faster than reaction (2), which therefore explains why In_2O_3 is the major product. The only remaining question is why the reaction products are amorphous in the cold reaction and why crystalline products are obtained under room-temperature conditions. We interpret these differences based on the Neppiras[28] hot spot mechanism in which T_{max}, the peak temperature generated during the collapse of a gas-filled cavity, is inversely proportional to the gas pressure inside the bubble at the initiation of the collapse. We have calculated the final temperature using Neppiras' formula

$$T_{max} = T_0\{P_a(\gamma - 1)/Q\}$$

where T_{max} and T_0 are the final and starting tempera-

(26) Sostaric, J. Z.; Caruso-Hubson, R. A.; Mulvaney, P.; Grieser, F. *J. Chem. Soc., Farady Trans.* **1997**, *93*, 1791.
(27) Yura, K.; Fredrikson, K. C.; Matijevic, E. *Colloids Surf.* **1990**, *50*, 281.
(28) Neppiras, E. A. *Phys. Rep.* **1980**, *61*, 159.

tures, respectively, P_a is the acoustic pressure at the intiation of the collapse, $\gamma = C_p/C_v$, and Q is the gas pressure in the bubble upon initiation of the collapse. Assuming P_a as 1 atm, we obtained T_{max} for the 0 °C and room-temperature reactions as 14 884 and 173 K, respectively. The bubble collapses in less than a nanosecond[30,31] and the cooling rates obtained are very high ($>10^{14}$ K/s) for the 0 °C reaction, not allowing the products to organize and crystallize. A much slower cooling rate is obtained for the room-temperature reaction in which only crystalline products are obtained. This will also affect the interface layer, where the temperature will be higher for the 0 °C reaction. These arguments have been discussed previousely by Suslick,[29] who has demonstrated that the higher cooling rates obtained during the collapse of the sonication bubble lead to the formation of amorphous products.

Acknowledgment. Prof. A. Gedanken thanks the NEDO International Joint Research Grant and the German Ministry of Science through the Deutsche-Israel program (DIP) for supporting this research. We all thank Dr. Shifra Hochberg for editorial assistance.

CM010162+

(29) Suslick, K. S.; Choe, S. B.; Cichowlas, A. A.; Grinstaff, M. W. *Nature* **1991**, *353*, 414.
(30) Hiller, R.; Putterman, S. J.; Barber, P. B. *Phys. Rev. Lett.* **1992**, *69*, 1182.
(31) Barber, P. B.; Putterman, S. J. *Nature* **1991**, *352*, 318.